Available online at www.sciencedirect.com
ScienceDirect
Journal of Bionic Engineering 6 (2009) 161–173

Max-Min Adaptive Ant Colony Optimization Approach to Multi-UAVs Coordinated Trajectory Replanning in Dynamic and Uncertain Environments

Hai-bin Duan, Xiang-yin Zhang, Jiang Wu, Guan-jun Ma

School of Automation Science and Electrical Engineering, *Beihang University*, *Beijing* 100191, *P. R. China*

Abstract

Multiple Uninhabited Aerial Vehicles (multi-UAVs) coordinated trajectory replanning is one of the most complicated global optimum problems in multi-UAVs coordinated control. Based on the construction of the basic model of multi-UAVs coordinated trajectory replanning, which includes problem description, threat modeling, constraint conditions, coordinated function and coordination mechanism, a novel Max-Min adaptive Ant Colony Optimization (ACO) approach is presented in detail. In view of the characteristics of multi-UAVs coordinated trajectory replanning in dynamic and uncertain environments, the minimum and maximum pheromone trails in ACO are set to enhance the searching capability, and the point pheromone is adopted to achieve the collision avoidance between UAVs at the trajectory planner layer. Considering the simultaneous arrival and the air-space collision avoidance, an Estimated Time of Arrival (ETA) is decided first. Then the trajectory and flight velocity of each UAV are determined. Simulation experiments are performed under the complicated combating environment containing some static threats and popup threats. The results demonstrate the feasibility and the effectiveness of the proposed approach.

Keywords: Multiple Uninhabited Aerial Vehicles (multi-UAVs), Ant Colony Optimization (ACO), trajectory replanning, collision avoidance, Estimated Time of Arrival (ETA)

doi: 10.1016/S1672-6529(08)60113-4

1 Introduction

Uninhabited Aerial Vehicle (UAV) is an inevitable trend of the modern aerial weapon equipments which develop in the direction of unmanned attendance and intelligence[1]. Research on UAV directly affects battle effectiveness of the air force. Trajectory planning is to generate a space path between an initial location and a desired destination that has an optimal or near-optimal performance under specific constraint conditions, which is an imperative task in the design of UAV. There are several considerations for an ideal trajectory planner, including optimality, completeness and computational complexity, which is also the most important requirement since trajectory planning has to occur quickly due to fast vehicle dynamics[2]. The current combating environments are not static but are constantly changing with many uncertain factors. In the air battlefield, there are not only a number of static threats which have been known a priori, but also others "pop up", or some threats that become known only when one UAV maneuvers into their proximity. Furthermore, even those static threats whose locations have been detected ahead of time, their threat grade or threat scope may change frequently, which also makes them uncertain. Considering these uncertain factors, the pre-planned trajectories often do not adapt to the changing air battlefield. In order to increase the survival chance of multiple Uninhabited Aerial Vehicles (multi-UAVs), the trajectory replanning is essential while encountering the popup threats[3–6]. Suppose maximizing the probability that the mission in dynamic and uncertain environments will succeed, it is desirable to assign multi-UAVs to conduct all the missions together[7], and thus the problem of multi-UAVs coordinated trajectory replanning is put forward.

Multi-UAVs coordinated trajectory replanning is to generate new trajectories from their current sites to the desired destinations after popup threats are detected. The new trajectories should have the optimal or near-optimal coordinated performance under specific constraints,

Corresponding author: Hai-bin Duan
E-mail: hbduan@buaa.edu.cn

which not only requires multi-UAVs to fly through enemy region safely but also demands multi-UAVs to reach their targets simultaneously or at a certain interval time, as well as to avoid various collisions[8].

Ant Colony Optimization (ACO) was firstly put forward by Colorni *et al*. in 1991[9], which was originally presented under the inspiration of the collective behavior study results on real ant system[10]. The inspiring source of ACO is the foraging behavior of real ants which enables them to find the shortest paths between nest and food sources[11]. The promising ant colony algorithm is a relatively new optimization technique, and also a model-based approach for solving many complicated combinatorial optimization problems[12]. It has been applied extensively to many NP-hard problems such as the Traveling Salesman Problem (TSP), the Job-shop Scheduling Problem (JSP), the Vehicle Routing Problem (VRP), the Graph Coloring Problem (GCP), the Quadratic Assignment Problem (QAP), and so on[13,14]. As for the UAV coordinated control field, this approach has also been applied to such problems as the target assignment[15], the path planning[16–19], formation control, and so on. However, the basic ACO model is easy to fall into local best, and the convergence speed is rather slow in solving complex problem.

In this paper, a novel coordinated trajectory replanning approach for multi-UAVs is proposed, which is based on the Max-Min adaptive ACO. The main characteristics of our proposed algorithm is that ants of each sub-population take both their own route information and that of other sub-populations as the colligate decision information. The coordination of multi-UAVs is considered mainly from two aspects:

(1) Simultaneous arrival, which requires determining an Estimated Time of Arrival (ETA) at the specific destinations[20]. Each UAV selects candidate trajectory, and adjusts the flight velocity corresponding to the ETA. Of course, the multi-UAVs trajectories and velocities will change coordinately when some popup threats occur.

(2) Collision avoidance, which requires that the trajectories of multi-UAVs should have no overlaps or crosses between each other.

The experimental results are also presented to verify that our approach is feasible and effective for solving the multi-UAVs coordinated trajectory replanning problems.

The remainder of this paper is organized as follows: Section **2** introduces the basic model of multi-UAVs coordinated trajectory replanning, which is divided into several sub-sections, including problem description, threat modeling, constraint conditions, coordinated function and coordination mechanism. Subsequently, the principle of our proposed Max-Min adaptive ACO algorithm and its application to multi-UAVs coordinated trajectory replanning are presented in Section **3**. Then, in Section **4**, several simulation experiments are conducted under various complicated combating environments. Our concluding remarks and future work are summarized in the last section.

2 Model of multi-UAVs coordinated trajectory replanning

2.1 Description of multi-UAVs coordinated trajectory replanning

Multi-UAVs coordinated trajectory planning is to generate a safe and short trajectory for each UAV. In addition, the trajectory should satisfy the requirements concerning multi-UAVs' coordinateness. Therefore, in the issue of multi-UAVs coordination, the planned trajectories may be not optimal for any individual vehicle, but they are required to be optimal or near optimal for the whole team[21].

Suppose that a formation of multi-UAVs is required to fly through the enemy territory and to attack the same or different known target locations. There are a number of threats in the flight environment, some of them are known a priori, whereas others popup or become known only when a UAV maneuvers into its proximity. We assume that each UAV is equipped with sensing capability so that they can detect the popup threats in their surroundings. We also assume that the multi-UAVs are equipped with a communication network, so they can inform other UAVs of the popup threats' information that they just detected. As shown in Fig. 1, the UAVs formation is commanded to attack an enemy objective. UAVs fly along their preplanned trajectories with respective flight velocity, and they are required to arrive at the same time given via planning. When one popup threat appears just on one UAV's flight route and poses a threat to it, the current trajectory is not feasible but even dangerous. At this moment, the UAV has to find other new trajectory. Meanwhile, in order to ensure that the multi-UAVs formation launch an attack simultaneously

and avoid collision, it is also necessary for other UAVs in the formation to adjust their respective trajectories, and thus, the coordinated trajectory replanning for the whole formation is inevitable. Moreover, along with the change of multi-UAVs' trajectory, the ETA is also confirmed again accordingly, as well as the flight velocity of each UAV.

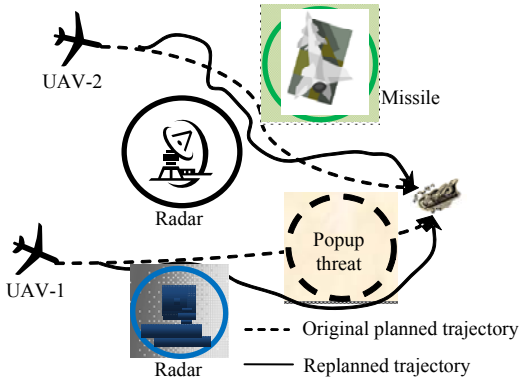

Fig. 1 Description of multi-UAVs coordinated trajectory replanning.

2.2 Threat sources modeling

Modeling of threat sources is the key task in multi-UAVs optimal trajectory replanning. In order to simplify the multi-UAVs trajectory replanning problem, the air battlefield can be divided into two-dimensional mesh, thus forming a two-dimensional network diagram connecting the starting point and goal point[15] (shown in Fig. 2). In this way, the problem of UAV optimal trajectory planning can be regarded as the general path optimization problem in essence.

In Fig. 2, suppose the flight mission for UAV is from node *B* to node *A*. There are some threatening areas in the battlefield. A coordinate system can be established with *OX* as the *x* axis and *OY* as the *y* axis, which covers the whole task region including the starting points, targets and all threatening regions that may pose threat to the UAV. Then, we divide *OX* into *m* sub-sections, and divide *OY* into *n* sub-sections equally. Thus, there are m+1 vertical lines and n+1 horizontal lines. Where the m+1 vertical lines can be labeled with L_1, L_2, …, L_{m+1}. The m+1 vertical lines and the n+1 horizontal lines cross-constitute (m+1) × (n+1) nodes. We name these nodes as $L_1(x_1,y_1)$, $L_2(x_2,y_1)$,…, $L_{m+1}(x_{m+1},y_1)$, … , $L_1(x_1,y_{n+1})$, … , $L_{m+1}(x_{m+1},y_{n+1})$, where $L_i(x_i, y_j)$ denotes the cross point of the *i*-th vertical line and the *j*-th horizontal line. In this way, the path from the starting point

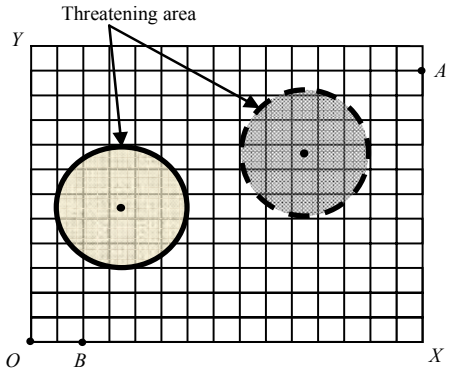

Fig. 2 Typical UAV battle field model.

B to the target point *A* can be described as follows[15,19]:

$$\text{Path} = \{B, L_{i_1}(x_{i_1}, y_{j_1}), L_{i_2}(x_{i_2}, y_{j_2}), \cdots, L_{i_k}(x_{i_k}, y_{j_k}), A\},$$

where $i_k = 1, 2, \ldots, m+1, j_k = 1, 2, \ldots, n+1$.

After the construction of the two-dimensional mesh covering the whole task region, the following work is to calculate the threat cost of each edge. As for those edges in the threatened ranges of enemy's radar and anti-aircraft weapons, the threat cost to be minimized in the trajectory planning is the received radar energy from the radar sites[22], which is:

$$J_{ij,\text{threat}} = \int_0^{L_{ij}} \sum_{k=1}^{N_t} \frac{1}{((x-x_k)^2 + (y-y_k)^2)^2} \mathrm{d}l, \quad (1)$$

where L_{ij} denotes the edge length linking the *i*-th and the *j*-th nodes in the generated mesh, (x_k, y_k) is the coordinate of the *k*-th threat source; N_t is the number of threats including radars, missiles and anti-aircraft guns that can pose threat to the edge (*i*, *j*). However, this equation is hard to calculate, so a computationally more efficient and acceptably accurate approximation to the exact solution is to calculate the threat cost at several locations along an edge and take the length of the edge into account. In this paper, the threat cost was calculated at five points along each edge[15,19], as shown in Fig. 3.

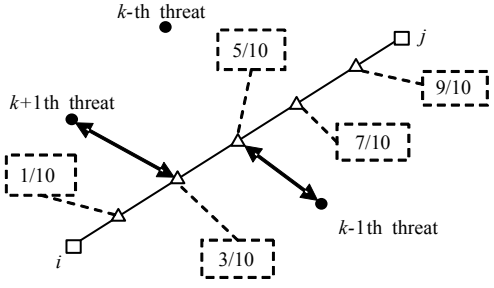

Fig. 3 Threat cost at five points along an edge.

The threat cost associated with the edge (i, j) is given by the following equation[1,4,15,17–19,21,23]:

$$J_{ij,\text{threat}} = L_{ij}\sum_{k=1}^{N_t} w_k\left(\frac{1}{d_{0.1,k}^4}+\frac{1}{d_{0.3,k}^4}+\frac{1}{d_{0.5,k}^4}+\frac{1}{d_{0.7,k}^4}+\frac{1}{d_{0.9,k}^4}\right), \quad (2)$$

where $d_{0.1,k}$ is the distance from the 1/10 point on the edge (i,j) to the k-th threat, w_k denotes a threat weighting coefficient, which is used to evaluate the threat grade of each threat source.

Moreover, it can simply consider the fuel cost J_{fuel} equals to the path length L, and thus, the fuel cost associated with each edge $J_{ij,\text{fuel}}$ is equal to L_{ij}. The total cost for traveling along the edge (i,j) comes from a weighted sum of the threat and fuel costs[1,4,15,17–19,21,23]:

$$J_{ij} = f\cdot J_{ij,\text{threat}} + (1-f)\cdot J_{ij,\text{fuel}} \quad (0 \leqslant f \leqslant 1). \quad (3)$$

The choice of f between 0 and 1 gives the designer certain flexibility to dispose relationships between the threat exposition degree and the fuel consumption. When f is closer to 0, a shorter path is needed in order to reduce the fuel consumption, with less attention paid to the radar's exposed threat. On the contrary, when f is closer to 1, it requires avoiding the threat as far as possible on the cost of sacrificing the trajectory length. For this work, a value of 0.75 was found to produce paths that were balanced in terms of threat avoidance and path length.

2.3 Constraints conditions of multi-UAVs coordinated trajectory replanning

Comparing with the trajectory planning of a single UAV, the difference of multi-UAVs coordinated path planning also lies in the constraint conditions that ought to be taken into account. Besides the physical properties and mission demands of a individual vehicle, the coordination and cooperation among various UAVs bring several extra co-constraints, including timing constraint that UAVs should reach objectives simultaneously, collision avoidance, and so on. Our work mainly involves the following three constraints:

(1) Minimum flight turning radius constraint: Considering the maneuverability of UAV, the turning radius in the generated trajectory must be larger than the minimum turning radius of each UAV, which means the planned trajectory should avoid larger turning. In this paper, we set the constraint on the choice of waypoint (node) as shown in Fig. 4.

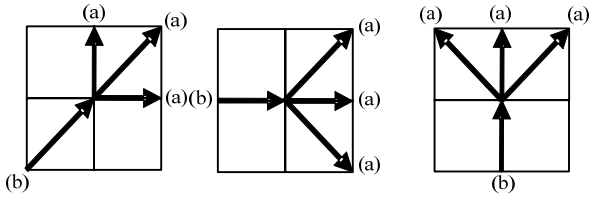

Fig. 4 Constraint on the node selection.

In Fig. 4, the center node in the square is the current site of the UAV, (b) is the last waypoint just before current one. Considering that UAV cannot take too big turning, next waypoint can only be selected from those points labeled with (a).

(2) Timing coordination constraint: Under this kind of coordination constraint, the goal is to decide the coordinated arrival time for multi-UAVs. The trajectory generated for multi-UAVs should ensure the multi-UAVs arriving at their respective targets simultaneously (as shown in Fig. 5). The multi-UAVs must minimize their exposure to threats under the constraint of simultaneous arrival. Therefore, we should comprehensively consider both the length of trajectory and UAVs' flight velocity to assign the team-optimal ETA for the multi-UAVs formation.

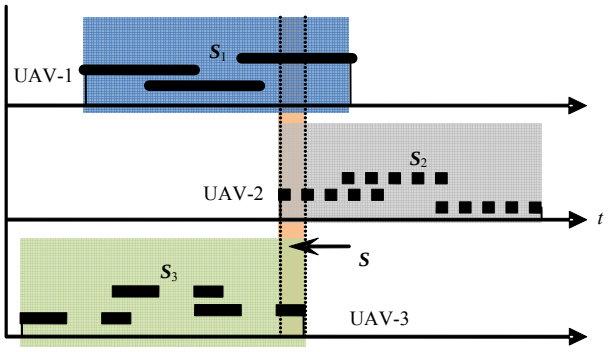

Fig. 5 Feasible region of arrival time.

Suppose that N UAVs participate in the flying mission. Each vehicle flies along its route with the velocity constraints $v\in[V_{\min}, V_{\max}]$. For the j-th trajectory planned for the i-th UAV, of which the length is labeled as $L_{i,j}$, we determine the range of its ETA as[5,8,20]:

$$T_{i,j} \in [\frac{L_{i,j}}{V_{\max}}, \frac{L_{i,j}}{V_{\min}}] \ . \quad (4)$$

We assume the i-th UAV has generated *num* candidate trajectories, and thus, its estimated time for arrival

is a union $\boldsymbol{S}_i$ determined as:

$$\boldsymbol{S}_i = [\frac{L_{i,1}}{V_{\max}}, \frac{L_{i,1}}{V_{\min}}] \cup [\frac{L_{i,2}}{V_{\max}}, \frac{L_{i,2}}{V_{\min}}] \cup \cdots \cup [\frac{L_{i,num}}{V_{\max}}, \frac{L_{i,num}}{V_{\min}}]. \quad (5)$$

As for the UAVs formation with N vehicles, the arrival time must be contained in the time intersection S as follows:

$$\boldsymbol{S} = \boldsymbol{S}_1 \cap \boldsymbol{S}_2 \cap \cdots \cap \boldsymbol{S}_N . \quad (6)$$

If $\boldsymbol{S}$ is not a void, assume such a time $T_a \in \boldsymbol{S}$, and each UAV must have at least one trajectory satisfying the arrival time T_a , and thus T_a can just be regarded as the ETA. By this method, it is available for multi-UAVs to satisfy the requirement of simultaneous arrival.

(3) Air collision avoidance constraint: Another coordination requirement concerned in multi-UAVs coordinated trajectory replanning is to reduce the risk of collision, which is so-called air-space coordination. Because our work is based on the 2-D space with the assumption that all individual UAVs fly at the same altitude, a proper approach to ensure that no collision will occur is to eliminate any overlap between two UAVs' trajectories[21]. It is clear that if the proportion of overlaps in the entire trajectory is bigger, the probability of collision is greater. Therefore, multi-UAVs' coordinated trajectory should ensure non-overlap as far as possible to implement air-space coordination.

2.4 Coordination function

In multi-UAVs coordinated trajectory replanning, the essential idea is that if each vehicle knows the coordination variable and responds appropriately, the coordinated behavior can be achieved. For the timing coordination constraint of simultaneous arrival introduced in the preceding section, the key coordination variable is the arrival time. That is to say, the key work of the multi-UAVs coordination is to select a proper factor from the time intersection $\boldsymbol{S}$ determined in Eq. (6) as the value of the coordination variable. To do this, it is necessary to construct the coordination function J_{co} to determine the coordination variable[8,20].

$$J_{\text{co},i,j}(T_{i,j}) = f_1 \cdot J_{i,j} + f_2 \cdot T_{i,j} , \quad (7)$$

where f_1 and f_2 are two constants, which may be the same or different for various UAVs. The variable $J_{i,j}$ denotes the cost of the j-th trajectory planned by the i-th UAV, which is determined by the equation $J_{i,j} = f \cdot J_{i,j,\text{threat}} + (1-f) \cdot J_{i,j,\text{fuel}}$ $(0 \le f \le 1)$, which is definite for a specific trajectory. Thus, the arrival time $T_{i,j}$ is the only independent variable determining $J_{\text{co},i,j}$. The entire cost of the multi-UAVs is:

$$J_{\text{co}} = \sum_{i=1}^{N} \sum_{j=1}^{Num} J_{\text{co},i,j}(T_{i,j}) . \quad (8)$$

Fig. 6 shows the relationship between $J_{\text{co},i,j}$ and $T_{i,j}$ for each trajectory[1]. As shown in Fig. 6, in order to minimize the entire coordination function, the coordinated arrival time T_a often selects the minimum of the feasible region, that is $T_a = \min S$.

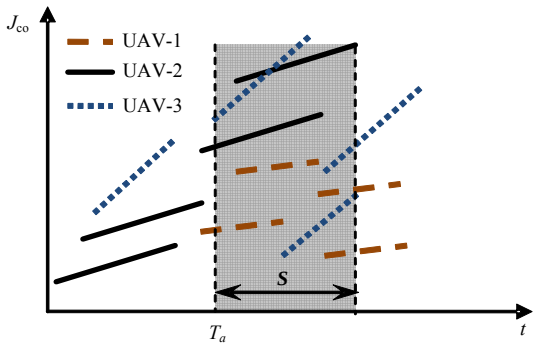

Fig. 6 Determination of the coordination variable.

2.5 Coordination mechanism of multi-UAVs trajectory replanning

The framework of the trajectory planning for a single UAV consists of three main layers: the coordination decider, the trajectory planner, and the trajectory smoother. The trajectory planner quickly calculates a series of safe enough straight-line trajectories. Communication between the trajectory planner and the coordination decider can help to generate candidate trajectories avoiding overlaps with those of other UAVs. These candidate trajectories are used by the coordination decider to determine coordination information such as the coordinated time. Because the straight-line trajectories produced by the trajectory planner are not dynamically feasible for the UAV to fly, the trajectory smoother is employed to generate flyable trajectories and send commands to the UAV autopilot. The function of the dynamic trajectory smoother is to smooth junctions in the trajectory with a sequence of radial arcs that the UAV can fly along. It is essential for timing-critical missions that the length of the original straight-line trajectory must be preserved in the smoothing process. Fig. 7 displays this mechanism.

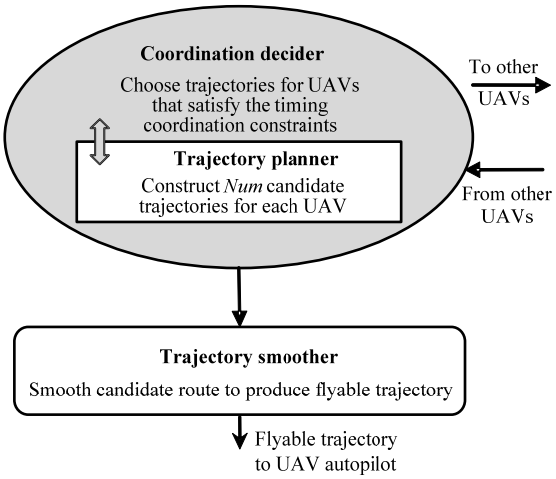

Fig. 7 Trajectory planning mechanism for a single UAV.

Fig. 8 describes the coordination mechanism of multi-UAVs trajectory replanning[8]. The framework is distributed, enabling each UAV to perform its own trajectory planning sub-systems. The algorithm implemented on each UAV in the coordination decider is identical. Multi-UAVs communicate the coordination information in the forms of coordination function and coordination variable in the coordination decider layer. Using the coordination information, multi-UAVs calculate the coordinated arrival time for the UAVs formation, which is just the ETA. After that, the coordination decider calculates the flying velocity for each UAV according to the generated trajectory and the ETA. Although only three UAVs are shown in Fig. 8, the distributed structure of the framework applies to larger numbers of multi-UAVs obviously.

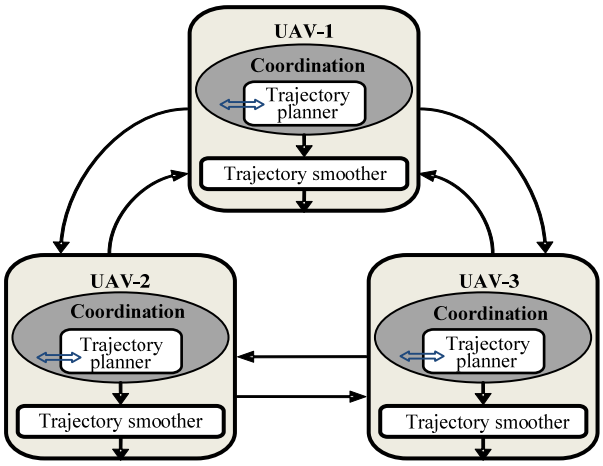

Fig. 8 Coordination mechanism of multi-UAVs trajectory replanning.

Furthermore, modern UAVs are equipped with the ability to detect their surroundings, so that they can sense the popup threats occurring in the mission region. The cause of trajectory replanning lies in following aspects: (1) the popup threat is detected just on the flight route ahead, and the vehicle has to change its route for security; (2) the UAV is not threatened by the popup threat, but in view of coordination, it also receives the command of replanning; (3) the mission changes. In this paper, the third cause is not involved. When the replanning is inevitable, information about the popup threats including the locations and threat grades will soon be shared by the multi-UAVs. Then, every UAV slows down or speeds up and flies to a neighboring safe node, which serves as the starting point of the following replanning. During the span, the new replanned trajectory is generated for multi-UAVs, and so is the new ETA. In the replanning procedure, on the basis of original edge cost of the 2-D mesh, the first step is to update the original threat cost of those edges threatened by popup threats, and recalculate their cost function value. Then multi-UAVs start to implement the coordinated trajectory replanning from the new starting points to their arranged targets. In this procedure as shown in Fig. 9, a set of new trajectories ought to be reproduced, and UAVs also should recalculate the ETA and re-adjust respective flight velocity. The procedure of trajectory replanning will perhaps be carried on more than once due to uncertain change of the complicate combating environment.

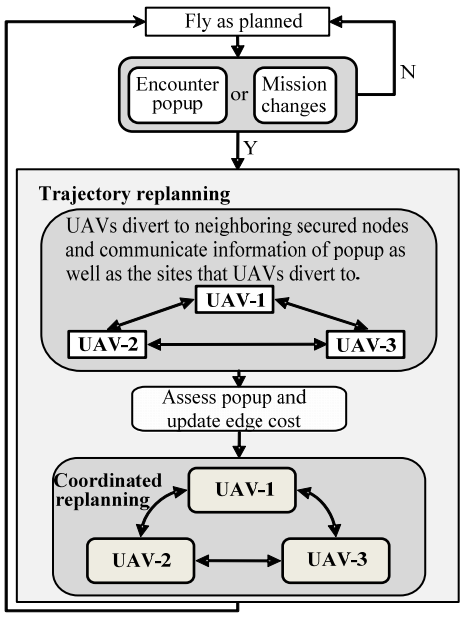

Fig. 9 Procedure of multi-UAVs trajectory replanning.

3 Max-Min adaptive ACO applied to multi-UAVs coordinated trajectory replanning

3.1 Principle model of ACO with improved strategies

The parallel mechanism of ACO mainly contains two basic processes: adaption and cooperation. In adaption process, the candidate solutions continue to readjust their structures on the basis of information accumulating. While in the cooperation stage, the candidate solutions exchange information to produce better solutions. ACO algorithm was inspired by the observation on ant colony foraging behavior[9], and on that ants can often find the shortest path between food source and their nest. The principle of this phenomenon is that ants deposit a chemical substance (called pheromone) on the ground, thus, they mark a path by the pheromone trail. In this process, a kind of positive feedback mechanism is adopted. An ant encountering a previously laid trail can detect the concentration of pheromone trail[10–13]. It decides with high probability to follow a shortest path, and reinforce the trail with its own pheromone. The larger amount of the pheromone is on a particular path, the higher probability that an ant selects that path and the path's pheromone trial will become denser. At last, the ant colony collectively marks the shortest path, which has the largest pheromone amount. Such simple indirect communication way among ants embodies actually a collective learning mechanism. Fig. 10 shows the principle that ants exploit pheromone to establish the shortest path from a nest to a food source and back.

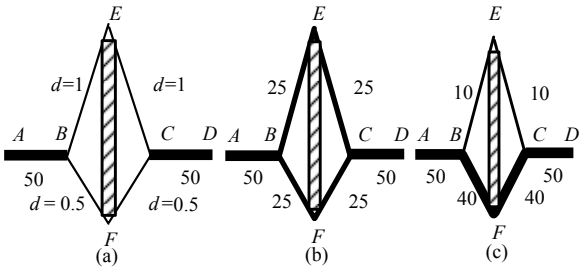

Fig. 10 Diagram of ant colony algorithm principle.

The ACO model was first applied to the TSP, which is to find the shortest closed loop that traverses all cities included exactly once. While the UAV path planning is to find the optimal or suboptimal safe flight trajectory, along which UAV is able to accomplish the prearranged task and avoid the hostile threats. There are some common points between TSP and UAV trajectory planning, and ACO is a feasible way in solving UAV trajectory planning problem under complicated combat field environment.

For the *i*-th vehicle in the formation of *N* UAVs, let *m* ants be in its starting point, the ants will choose the next nodes in the grid network according to the transition rule. An ant left pheromone which can be felt by the next ant as a signal to affect its action, and the pheromone which the following one left will enhance the original pheromone. Thus, the more ants a mesh edge is passed by, the higher possibility that the edge can be selected by other ants. This process can guarantee nearly all ants walk along the shortest UAV path in the end.

The key factors in ACO affecting the ants' behaviors are the pheromone τ and the heuristic desirability η. In our work, we described the heuristic desirability from node *s* to node *u* as:

$$\eta_{su} = \frac{1}{J_{su} \cdot d_{u,\text{target}}}, \tag{9}$$

where, J_{su} is the total cost of the edge (*s*, *u*), and $d_{u,\text{ target}}$ represents the distance from node *u* to the target, which is used to lead ants located at node *s* tend to choose those nodes that are nearer to the target.

The amount of pheromone trail τ that leads ants choose next node consists of two parts in our work: one is the traditional edge pheromone τ^e, the other is the point pheromone τ^p defined for the collision avoidance consideration. Ant colonies not only leave their pheromone on the edges they passed, but also deposit the pheromone on those nodes in their paths. Ants serving for the *i*-th UAV will tend to choose those edges richer in its own edge pheromone τ_i^e and avoid the nodes with bigger point pheromone of other UAVs. Thus, total pheromone considered by the *i*-th UAV's ants from node *s* to *u* is determined by:

$$\tau_{i,su} = \tau_{i,su}^e \cdot \frac{N-1}{\sum_{j \neq i} \tau_{j,u}^p}. \tag{10}$$

We define the transition probability from node *s* to node *u* for the *k*-th ant as[9]:

$$p_{i,su}(t) = \begin{cases} \dfrac{[\tau_{i,su}(t)]^\alpha [\eta_{su}]^\beta}{\sum_{v \in allowed_k} [\tau_{i,sv}(t)]^\alpha [\eta_{sv}]^\beta} & if \quad u \in allowed_k \\ 0 & \text{otherwise} \end{cases}, \tag{11}$$

where $allowed_k$ denotes the feasible domain of the k-th ant. α and β are the parameters that control the relative importance of trail versus visibility.

After the ants in the algorithm construct their paths, the edge pheromone trail values of every edge (s, u) and the point pheromone of every point u are updated according to the following equations:

$$\tau^e_{i,su}(t+1) = (1-\rho)\cdot\tau^e_{i,su}(t) + \Delta\tau^e_{i,su}, \quad (12)$$

$$\tau^p_{i,u}(t+1) = (1-\rho)\cdot\tau^p_{i,u}(t) + \Delta\tau^p_{i,u}, \quad (13)$$

where $\rho \subset (0, 1)$ is the local pheromone decay parameter, which represents the evaporation rate of trail between time t and t+1.

$$\Delta\tau^e_{i,su} = \sum_{k=1}^{n}\Delta\tau^e_{i,su,k}, \quad (14)$$

$$\Delta\tau^p_{i,u} = \sum_{k=1}^{n}\Delta\tau^p_{i,u,k}, \quad (15)$$

where $\Delta\tau^e_{i,su,k}$ and $\Delta\tau^p_{i,u,k}$ are the quantities of pheromone trail laid on edge (s, u) and the node u by the k-th ant of the i-th UAV between time t and t+1. In the popular ant-cycle model, they can be given by:

$$\Delta\tau^e_{i,su,k} = \begin{cases} \dfrac{Q}{J_{i,k}}, & if \quad k-\text{th ant uses } (s,u) \\ 0, & \text{otherwise} \end{cases}, \quad (16)$$

$$\Delta\tau^p_{i,u,k} = \begin{cases} \dfrac{Q}{J_{i,k}}, & if \quad k-\text{th ant uses node } u \\ 0, & \text{otherwise} \end{cases}, \quad (17)$$

where Q is a constant, and $J_{i,k}$ denotes the path cost of the k-th ant.

3.2 Max-Min adaptive ACO

In order to enhance performance of ant system, alleviate the problems concerning early stagnation and expedite the rapidity of convergence, the following strategies are introduced into the ACO algorithm.

(1) For the m ants serving for the i-th UAV, there are total m paths constructed in each iteration. The average cost of these paths is $J_{i,\text{ave}}(t) = \dfrac{1}{m}\sum_{k=1}^{m} J_{i,k}(t)$, when and only when the path cost of k-th ant in the t-th iteration satisfies $J_{i,k}(t) \leqslant J_{i,\min}(t)$, can the k-th ant update both its edge and point pheromone by Eqs. (16) and (17).

(2) Independent of the choice between the iteration-best and the global-best ant for the pheromone trail update, search stagnation may occur. Such a stagnation situation should be avoided. One way for achieving this is to influence the probability for choosing the next solution component, which depends directly on the pheromone trails and the heuristic information. The heuristic information is typically problem-dependent and static throughout the application of the algorithm. But by limiting the influence of the pheromone trails one can easily avoid the relative differences between the pheromone trails during the employment of the algorithm. To achieve this goal, ACO imposes and explicitly limits $\tau_{\max}$ and $\tau_{\min}$ on the minimum and maximum pheromone trails such that for all pheromone trails[24]. After updating pheromone in the end of iteration, following operation will be applied to the pheromone on both edges and points[24]:

$$\tau^{\text{new}}(t) = \begin{cases} \tau_{\min}, & \tau^{\text{old}}(t) < \tau_{\min} \\ \tau^{\text{old}}(t), & \tau_{\min} \leq \tau^{\text{old}}(t) \leq \tau_{\max} \\ \tau_{\max}, & \tau^{\text{old}}(t) > \tau_{\max} \end{cases}. \quad (18)$$

3.3 Application of Max-Min adaptive ACO to multi-UAVs coordinated trajectory replanning

The flowchart in Fig. 11 describes the detailed procedure of applying the proposed Max-Min adaptive ACO to a single UAV in the practical issue of multi-UAVs coordinated trajectory replanning. Ants of the i-th UAV have constructed their paths and finished updating both the edge and point pheromone trails. Then, the new updated pheromone is passed to the next iteration. Meanwhile, the point pheromone is transmitted to other UAVs. The multi-UAVs' air-space coordination which is mainly to deal with the collision avoidance just depends on the point pheromone. Therefore, through the communication of each UAV's point pheromone, the air-space coordination can be settled in the trajectory planner layer.

A series of feasible candidate routes have been determined for each UAV by the coordinated ACO, but it remains to select which trajectory each UAV will fly. In our work, from each sub-population we selected four optimal candidate trajectories for each UAV, then, determined the optimal coordination ETA by means of finding the coordination variable T_a that minimizes the total coordination cost. After gaining the team's

coordinated ETA, the trajectories that multi-UAVs will fly are available, so are the flight velocities of the UAVs. The complete procedure of applying ACO to the multi-UAVs coordination issue is shown in Fig. 12.

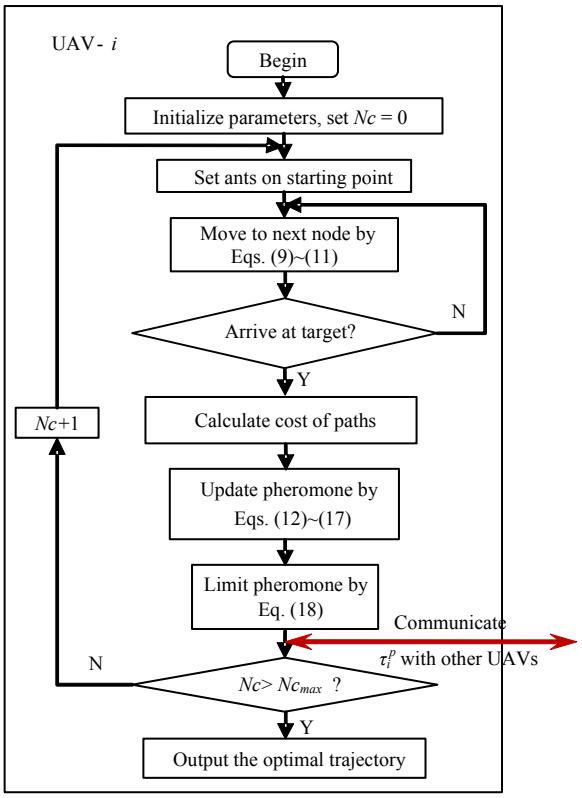

Fig. 11 Flowchart of Max-Min adaptive ACO applied to one UAV of multi-UAVs.

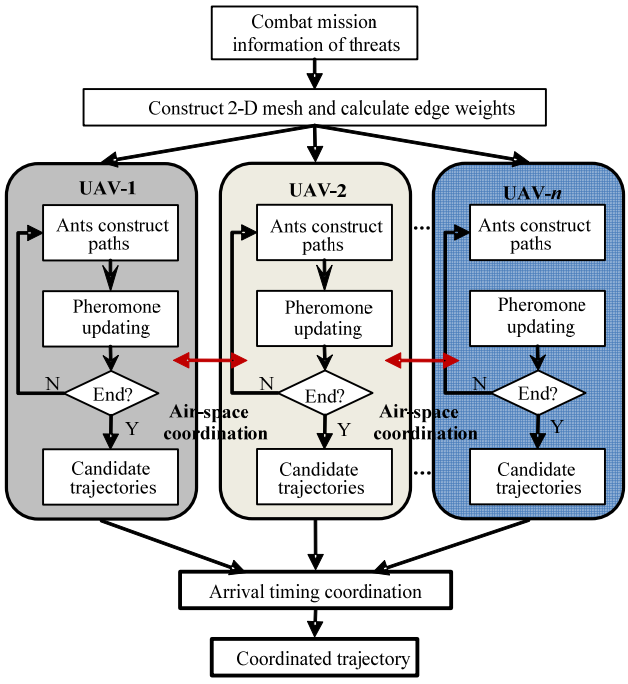

Fig. 12 Flowchart of multi-UAVs coordination using ACO.

The programming steps of the Max-Min adaptive ACO algorithm in solving trajectory replanning can be described as follows:

Step 1: Construct the 2-D mesh covering the mission region and calculate the cost of the edges.

Step 2: Initialize the parameters of the algorithm, including α, β, ρ, Q, τ_{max}, τ_{min}, as well as the number of ants m and the number of iteration Nc_{max}.

Step 3: Initialize the edge and point pheromones for every sub-population and place ants at the respective starting point.

Step 4: For each UAV, ants choose the node according to Eq. (6) until reach the target, and then some feasible trajectories are constructed at last.

Step 5: Calculate the cost function value $J_{i,k}$ of the k-th ant belonging to the i-th UAV, and update the point and edge pheromones according to Eqs. (12) ~ (17).

Step 6: Pass the pheromone on to next iteration calculation and communicate the point pheromone with other UAVs; then return to Step 4 until it satisfies the ending condition $Nc > Nc_{max}$.

Step 7: Select several feasible candidate routes for each UAV, and determine the optimal coordinated ETA for the team.

Step 8: According to the team ETA, select the trajectory and the flight velocity for each UAV.

When the popup threats are detected and the original trajectory is in danger, emergent response action of multi-UAVs will be taken according to the following steps:

Step 1: Determine the information of the popup threats, including the location, threatened range and threat grade.

Step 2: Calculate the threat cost of the edges which the popup threats pose to, and then update the cost function value of each edge in the 2-D mesh.

Step 3: Each UAV diverts to a neighboring and safe enough node, which will be taken as the new starting point of trajectory replanning.

Step 4: When multi-UAVs are moving as Step 3, the newly replanned trajectory is calculated according to the procedure shown in Fig. 11 and Fig. 12.

4 Simulation experiments

In order to investigate the feasibility and effectiveness of the proposed Max-Min adaptive ACO approach to multi-UAVs coordinated trajectory replanning,

a series of simulation experiments were conducted. These simulation experiments were all implemented in Matlab (Version 7.0) programming environment on an Intel Core 2 PC running Windows Vista, no ACO or multi-UAVs tools were used in the following experiments.

In these simulation experiments, the mission region is 60 km long and 70 km wide with five known enemy threats. Information about these hazarded threats is given in Table 1.

In the first experiment, two UAVs are assigned to reach the same target from neighboring nodes. In this scenario, only air-space coordination was considered in order to verify the collision avoidance performance of the Max-Min adaptive ACO model. Trajectories optimized in these experiments are presented in Fig. 13, and it is clear that there is no overlap between the two neighboring trajectories, thus the collision avoidance is achieved. Fig. 14 shows the evolution of the costs of two UAVs trajectories, which converge after a few iterations. The simulation results demonstrate that the ACO considering the point pheromone as air-space coordination factor is feasible to produce the trajectories satisfying collision avoidance.

In the second experiment, an air combat formation, composed of three UAVs and located on different sites, is assigned to attack different targets simultaneously. Table 2 shows the mission starting points and attacking targets.

Table 1 Information about known threats

No.	Location (km)	Threat radius (km)	Threat grade
1	(52,32)	10	2
2	(36,26)	6	1.2
3	(22,48)	8	1.6
4	(26,56)	12	1.4
5	(30,30)	9	2

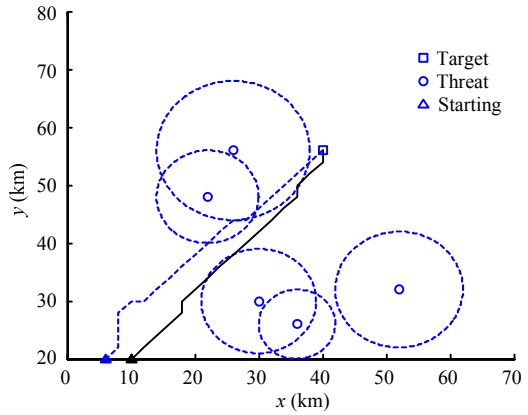

Fig. 13 Trajectories of two UAVs.

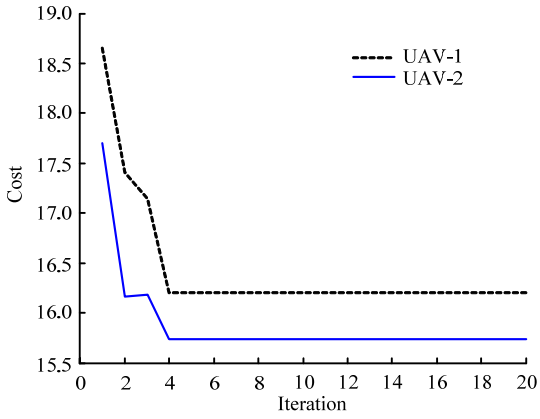

Fig. 14 Evolution curves of two UAVs trajectories' costs using the Max-Min adaptive ACO.

Table 2 Mission starting points and attacking targets

	UAV-1	UAV-2	UAV-3
Starting point (km)	(6,20)	(24,20)	(40,20)
Target (km)	(10,68)	(40,60)	(50,68)

The flight velocity is between $V_{max} = 300\ m{\cdot}s^{-1}$ and $V_{min} = 200\ m{\cdot}s^{-1}$. The initial parameters are: $\alpha = 3$, $\beta = 2$, $\rho = 0.7$, $Q = 10$, $Nc_{max} = 20$, $m = 20$, $\tau_{max} = 10$ and $\tau_{min} = 0.1$.

After iterated calculation, each UAV obtains four candidate trajectories. The determined arrival time ETA is shown in Fig. 15, in which, $T_a = 173$ s. According to this ETA, each UAV can select its optimized trajectory and proper flight velocity. The selected trajectory length and flight velocity are listed in Table 3.

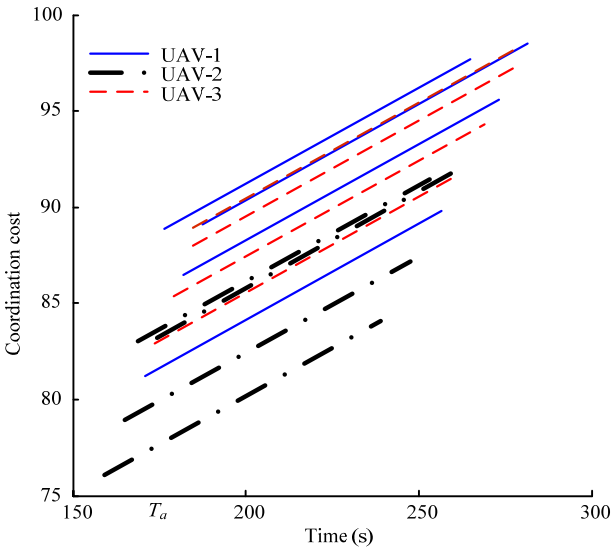

Fig. 15 Decision of ETA.

The original trajectories planed for three UAVs are shown in Fig. 16, while the evolution curves are shown in Fig. 17.

As shown in Fig. 18, two popup threats appear suddenly, which are detected by marching multi-UAVs. Information about these popup threats is shared immediately (Table 4).

Then, each UAV diverts to a neighboring secure node, which is taken as the new starting point. Meanwhile, computers equipped in UAVs run the replanning program and generate new trajectories for the UAVs.

Table 3 Arrival time, trajectory length and flight velocity planned for multi-UAVs

	UAV-1	UAV-2	UAV-3
ETA (s)		174	
Trajectory length (km)	51.31	47.80	52.14
flight velocity (km·s^{-1})	295	275	300

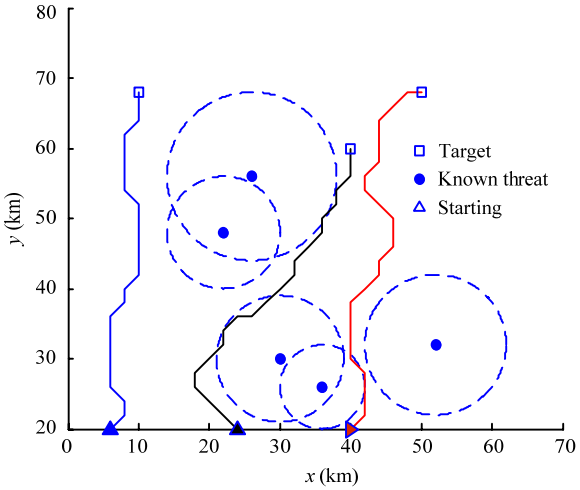

Fig. 16 Preplanned trajectories of three UAVs.

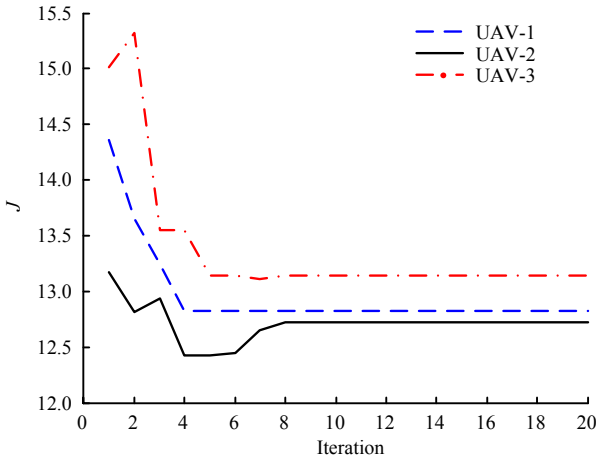

Fig. 17 Evolution curves of three UAVs using ACO.

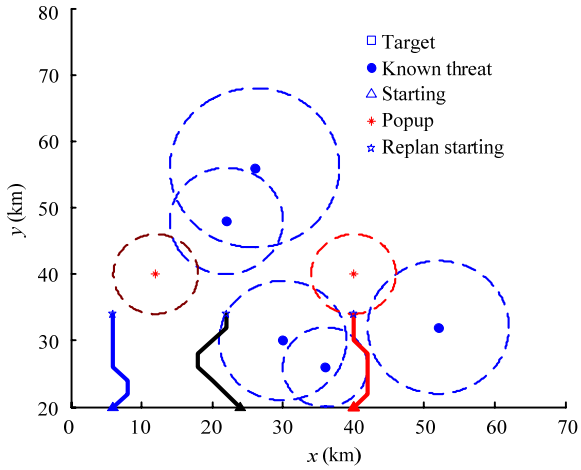

Fig. 18 Popup threats are detected by marching three UAVs.

Table 4 Information about popup threats

No.	Location (km)	Threat radius (km)	Threat grade
1	(12,40)	6	2.5
2	(40,40)	6	2

Comparison between the original trajectories and the new replanned trajectories is shown in Fig. 19. Fig. 20 shows the practical trajectories which the UAVs fly along in the air battlefield.

Figs. 21 to 23 show the results of another experiment. Different from the above two experiments, in this experiment the two UAVs have a common target. Because the original preplanned trajectories are hardly menaced by the popup threats, the replanned trajectories change little compared with the original ones.

The experimental results illustrate that the proposed Max-Min adaptive ACO algorithm can effectively solve multi-UAVs coordinated trajectory replanning problems and the convergence time is also rather short.

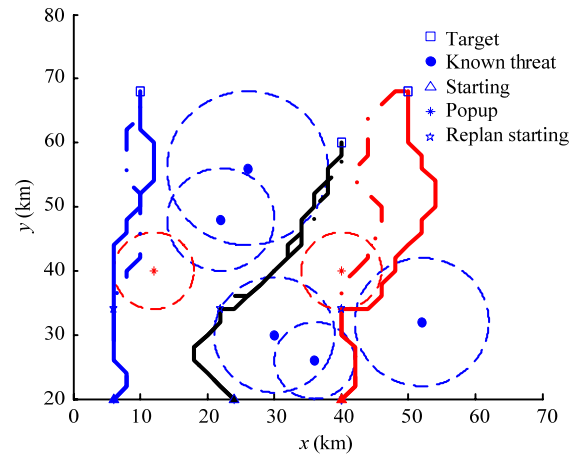

Fig. 19 Comparison between the original trajectories and the new replanned trajectories.

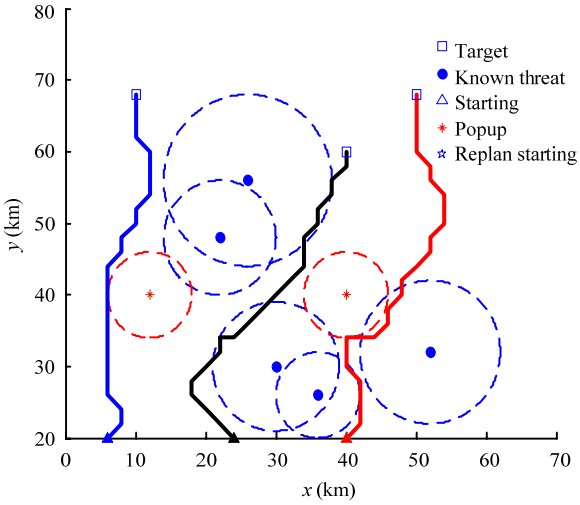

Fig. 20 Practical trajectories of three UAVs.

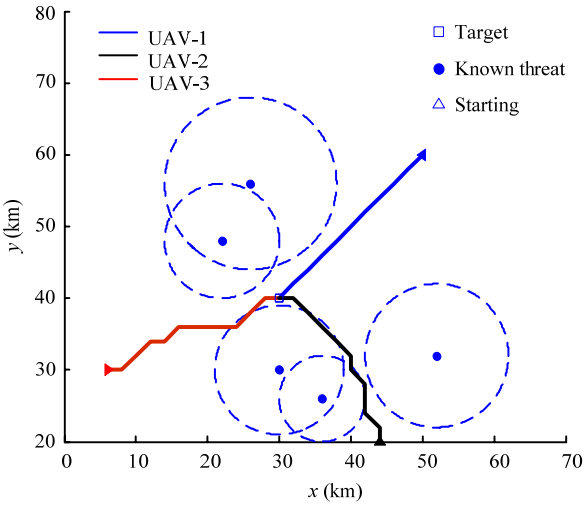

Fig. 21 Original trajectories of two VAUs with a common target.

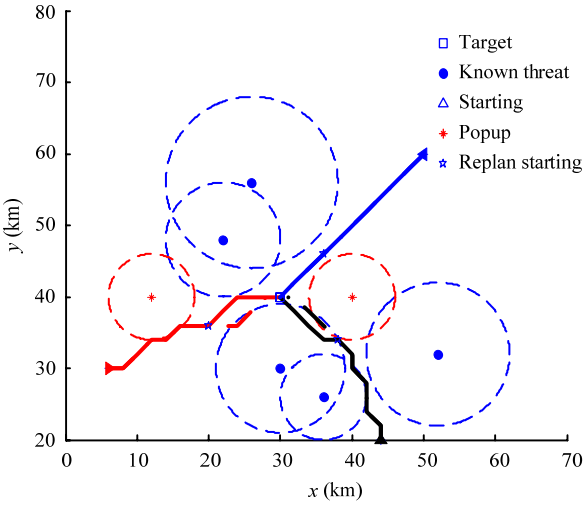

Fig. 22 Comparison between original and new trajectories.

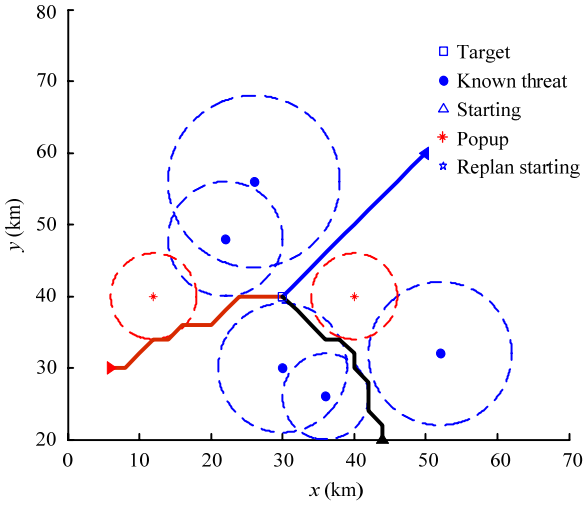

Fig. 23 Practical trajectories of two UAVs with common target.

5 Conclusions and future work

This paper focuses on a new Max-Min adaptive ACO method for the multi-UAVs coordinated trajectory replanning in dynamic and uncertain environments. This approach is based on multi-UAVs coordination mechanism and trajectory replanning strategy. Coordination between multi-UAVs includes two aspects: air-space collision avoidance and simultaneous arrival. The point pheromone in this approach takes effect in multi-UAVs' collision avoidance. The feasible team ETA helps the whole multi-UAVs formation to arrive all targets simultaneously. Simulation results verified the feasibility and effectiveness of the proposed ACO algorithm.

Future work will focus on applying the proposed ACO algorithm to multi-UAVs formation control and optimal formation reconfiguration under complicated dynamic environments.

Acknowledgement

This work was supported by the Natural Science Foundation of China (Grant no. 60604009), Aeronautical Science Foundation of China (Grant no. 2006ZC51039, Beijing NOVA Program Foundation of China (Grant no. 2007A017), Open Fund of the Provincial Key Laboratory for Information Processing Technology, Suzhou University (Grant no KJS0821), and "New Scientific Star in Blue Sky" Talent Program of Beihang University of China.

The authors are grateful to the anonymous referees for their valuable comments and suggestions.

References

[1] Beard R W, Mclain T W, Goodrich M A, Anderson E P. Coordinated target assignment and intercept for unmanned air vehicles. *IEEE Transactions on Robotics and Automation*, 2002, **18**, 911–922.

[2] Ben-Asher Y, Feldman S, Gurfil P, Feldman M. Distributed decision and control for cooperative UAVs using *Ad Hoc* communication. *IEEE Transactions on Control Systems Technology*, 2008, **16**, 511–517.

[3] Cowlagi R V, Tsiotas P. Multiresolution path planning with wavelets: A local replanning approach. *Proceedings of American Control Conference*, Washington, USA, 2008, 1220–1225.

[4] Chen Y M, Chang S H. An agent-based simulation for multi-UAVs coordinative sensing. *International Journal of Intelligent Computing and Cybernetics*, 2008, **1**, 269–284.

[5] Zheng C W, Ding M Y, Zhou C P. Cooperative path planning for multiple air vehicles using a co-evolutionary algorithm. *Proceedings of the First International Conference on Machine Learning and Cybernetics*, Beijing, China, 2002, 219–224.

[6] Zucker M, Kuffner J, Branicky M. Multipartite RRTs for rapid replanning in dynamic environments. *Proceedings of IEEE International Conference on Robotics and Automation*, Roma, Italy, 2007, 1603–1609.

[7] Beard R W, Mclain T W. Multiple UAV cooperative search under collision avoidance and limited range communication constraints. *Proceedings of IEEE Conference on Decision and Control*, Hawaii, USA, 2003, 25–30.

[8] Mclain T W, Beard R W. Coordination variables, coordination functions, and cooperative-time missions. *Journal of Guidance*, *Control*, *and Dynamics*, 2005, **28**, 150–161.

[9] Colorni A, Dorigo M, Maniezzo V. Distributed optimization by ant colonies. *Proceedings of European Conference on Artificial Life*, Paris, France, 1991, 134–142.

[10] Dorigo M, Gambardella L M. Ant colony system: A cooperative learning approach to the traveling salesman problem. *IEEE Transactions on Evolutionary Computation*, 1997, **1**, 53–66.

[11] Dorigo M, Maniezzo V, Colorni A. The ant system: Optimization by a colony of cooperating agents. *IEEE Transactions on Systems*, *Man*, *and Cybernetics-Part B*, 1996, **26**, 29–41.

[12] Bonabeau E G, Dorigo M, Theraulaz G. Inspiration for optimization from social insect behavior. *Nature*, 2000, **406**, 39–42.

[13] Duan H B. *Ant Colony Algorithms*: *Theory and Applications*, Science Press, Beijing, China, 2005. (in Chinese)

[14] Duan H B, Wang D B, Yu X F. Grid-based ACO algorithm for parameters tuning of NLPID controller and its application in flight simulator. *International Journal of Computational Methods*, 2006, **3**, 163–175.

[15] Duan H B, Ding Q X, Chang J J. Multi-UCAVs Task assignment simulation platform based on parallel ant colony optimization. *Acta Aeronautica ET Astronautica Sinica*, 2008, **29**, s192–s197. (in Chinese)

[16] Duan H B, Yu Y X, Zhou R. UCAV path planning based on Ant Colony Optimization and satisficing decision algorithm. *Proceedings of IEEE Congress on Evolutionary Computation*, Hong Kong, 2008, 957–962.

[17] Liu C G, Li W J, Wang H P. Path planning for UAVs based on ant colony. *Journal of Air Force Engineering University*, 2004, **2**, 9–12. (in Chinese)

[18] Ma G J, Duan H B, Liu S Q. Improved ant colony algorithm for global optimal trajectory planning of UAV under complex environment. *International Journal of Computer Science and Applications*, 2007, **4**, 57–68.

[19] Yu Y X, Duan H B, Zhang X Y. Three-dimension path planning for UCAV using hybrid meta-heuristic ACO-DE algorithm. *Proceedings of Asia Simulation Conference—7th International Conference on System Simulation and Scientific Computing*, Beijing, China, 2008, 919–924.

[20] Zheng C W, Li L, Xu F J, Sun F C, Ding M Y. Evolutionary route planner for unmanned air vehicles. *IEEE Transactions on Robotics*, 2005, **21**, 609–620.

[21] Ye Y Y, Min C P. A co-evolutionary method for cooperative UAVs path planning. *Computer Simulation*, 2007, **24**, 37–39. (in Chinese)

[22] Chandler P R, Rasmussen S, Pachter M. UAV cooperative path planning. *Proceedings of the AIAA Guidance*, *Navigation and Control Conference*, Denver, CO, 2000, AIAA-2000-4370.

[23] Xiao Q K, Gao X G. Study on a kind of local path replanning algorithm for UAVs. *Journal of Air Force Engineering University*, 2006, **24**, 67–80. (in Chinese)

[24] Thomas S, Holger H H. Max-Min ant system. *Future Generation Computer Systems*, 2000, **16**, 889–914.